Third International Conference on Inverse Design Concepts and Optimization in Engineering Sciences (ICIDES-III), Editor: G.S. Dulikravich, Washington D.C., October 23-25, 1991.

THE TURBOMACHINE BLADING DESIGN USING $S2$-$S1$ APPROACH

T. S. LUU*, Dr., Senior Researcher
L. BENCHERIF*, Graduate student
B. VINEY*, Dr., Engineer
J.M. NGUYEN DUC**, Engineer

*LIMSI (CNRS), BP 133
F 91403 ORSAY CEDEX, FRANCE

**SEP, BP 802
F 27207 VERNON, FRANCE

SUMMARY

The boundary conditions corresponding to the design problem when the blades being simulated by the bound vorticity distribution are presented. The 3D flow is analyzed by the two steps $S2 - S1$ approach. In the first step, the number of blades is supposed to be infinite, the vortex distribution is transformed into an axisymmetric one, so that the flow field can be analyzed in a meridional plane. The thickness distribution of the blade producing the flow channel striction is taken into account by the modification of metric tensor in the continuity equation. Using the meridional stream function to define the flow field, the mass conservation is satisfied automatically. The governing equation is deduced from the relation between the azimuthal component of the vorticity and the meridional velocity. The value of the azimuthal component of the vorticity is provided by the hub to shroud equilibrium condition. This step leads to the determination of the axisymmetric stream sheets as well as the approximate camber surface of the blade. In the second step, the finite number of blades is taken into account, the inverse problem corresponding to the blade to blade flow confined in each stream sheet is analyzed. The momentum equation implies that the free vortex of the absolute velocity must be tangential to the stream sheet. The governing equation for the blade to blade flow stream function is deduced from this condition. At the beginning, the upper and the lower surfaces of the blades are created from the camber surface obtained from the first step with the assigned thickness distribution. The bound vorticity distribution and the penetrating flux conservation applied on the presumed blade surface constitute the boundary conditions of the inverse problem. The detection of this flux leads to the rectification of the geometry of the blades.

NOMENCLATURE

Γ	circulation
V_o	upstream velocity
h	pitch of the cascade
α	inlet angle
β	outlet angle
ϕ	potential function
ψ	stream function
$f(x)$, $f(m,\psi)$	bound vortex distribution function, or loading function
dl	tangential displacement
ϑ	camber line inclination angle with respect to the meridional plane
x, y	Cartesian coordinates
z, θ, r	cylindrical coordinates
ξ^1, ξ^2, ξ^3	body fitted curvilinear coordinates
g	determinant of the metric tensor
g_{ij}	metric tensor elements
N_b	number of blades in the rotor or stator
$r\delta\theta_e$	thickness of the blade measured in the azimuthal direction
$\tilde{g}_{22}$	modified g_{22} simulating flow channel striction
$\tilde{g}$	determinant of the modified metric tensor (flow channel striction)
ρ	density
U^1, U^2, U^3	contraviant components of the absolute or relative velocity
$\vec{V}$	absolute velocity
$\vec{W}$	relative velocity
V_θ	azimuthal component of the absolute velocity
m	meridional streamwise curvilinear abscissa

Third International Conference on Inverse Design Concepts and Optimization in Engineering Sciences
(ICIDES-III), Editor: G.S. Dulikravich, Washington D.C., October 23-25, 1991.

$\vec{\omega}$	angular velocity of the rotor
p	pressure
p_t	total pressure
H	stagnation enthalpy or p_t/ρ
I	rothalpy or $H + \omega(V_\theta)$
$\vec{F}_b$	blade force
$\vec{F}_d$	dissipative force
η	efficiency
x^1, x^2	transformed coordinates system in S1 approach
Subscripts	
le	leading edge
te	trailing edge
o	reference
t	tangentiel component
n	normal component
i,k	nodal point indices
Superscripts	
$+$	upper side of the blade
$-$	lower side of the blade

1. INTRODUCTION.

Most of the blading design procedures consider the velocity distribution on both sides of the blade as the initial data, the inverse problem becomes ill-posed and the designer loses the control of thickness distribution of the blade. To overcome this deficiency, this paper suggests an inverse method by representing the blades by a distribution of bound and free vortices which produce the desired swirl ($V_\theta r$) variation. By introduction of the notion of associated elements on both sides of the blade in respect of the thickness distribution, and by imposing a conservative flux penetration through each pair of the associated elements when the geometry of the blade is not yet well defined, we obtain the well-posedness of the inverse problem. The iterative rectification of the camber surface in order to cancel the flow penetration leads to the final geometry of the blade. Treating first the 2D cascade design, §2 is devoted to show how to get the well posed inverse problem with the appropriate boundary conditions applied on the presumed blade contour, and the procedure leading to the rectification of the camber line related to the penetrating flux of the fluid determined on both sides of the blade. To treat the quasi 3D design, the S2 and S1 approach as proposed by C.H. Wu [1] is adopted. The loading produced by the velocity difference between the two faces of the blade is directly related to the bound vorticity distribution that the blade has to generate. Assuming the number of blades infinite, the vortex distribution as well as the flow field become axisymmetric (S2 flow), §3 shows how the blade thickness distribution and the loading distribution can be taken into account in this scheme, and how to deduce the pressure distribution on the blades when their number is finite. An application to the case of the centrifugal impeller is presented. The loss scheme by the introduction of a plausible value of efficiency η for each streamline as suggested by J.H. Horlock [2] is used. This approach opens up possibilities for the elaboration of a design which maintains the assigned value of the total pressure gain in each stage by modifying the ($V_\theta r$) distribution in free space between blade rows. §4 is devoted to the blade to blade flow (S1) inverse problem, the boundary conditions for 2D inverse problem are transposed to this quasi-3D flow. The stream function is used to define the flow field and the finite volume method is used to solve the problem. Examples show the results concerning the design of centrifugal impeller.

2. INVERSE PROBLEM FOR THE 2D CASCADE.

Figure 1 shows the geometry of the blade characterized by its thickness distribution and the shape of its camber line. The arc elements taken respectively on the upper side and the lower side tangential to two inscribed circles centered on the camber line at $x - dx/2$ and $x + dx/2$ are called associated to the camber line element. The center of these associated elements are characterized by the abscissa x of the camber line element. Let V_o represent the upstream velocity, h the pitch of the cascade, α and β the inlet and outlet flow angles, the circulation Γ of the bound vortex generated by the blade is given by:

Third International Conference on Inverse Design Concepts and Optimization in Engineering Sciences (ICIDES-III), Editor: G.S. Dulikravich, Washington D.C., October 23-25, 1991.

$$\Gamma = V_o h(\sin\alpha - \cos\alpha \tan\beta)$$

The bound vortex distribution on the blade can be represented by the function $\Gamma f(x)$, where $f(x)$ has to be a monotonic increasing function of x for the inverse problem: $f(x_{le}) = 0$, $f(x_{te}) = 1$ and $df/dx \geq 0$ defines the local loading. Figure 2 shows the typical form of the function $f(x)$, $df/dx = 0$ must be imposed near the trailing edge in order to obtain the zero loading according to the Kutta-Joukowsky condition; when the zero loading condition is imposed near the leading edge, the design will give a blade with adapted leading edge. The flow field can be represented by the velocity potential ϕ or by the stream function ψ, the assignment of the bound vortex distribution leads respectively to the following boundary condition applied on the associated elements on both sides of the blade [3]:

$$[\phi]_-^+ = \Gamma f(x) \qquad \text{or} \qquad [\frac{\partial \psi}{\partial n} dl]_-^+ = \Gamma \frac{df}{dx} dx \tag{2.1}$$

As the boundary condition is imposed on the presumed contour of the blade, the penetration of the fluid must be admitted., In order that the boundary condition does not produce extra flux, the flux penetration through each pair of associated elements is to be conservative, this implies:

$$[\frac{\partial \phi}{\partial n} dl]_-^+ = 0 \qquad \text{or} \qquad [\psi]_-^+ = 0 \tag{2.2}$$

The solution of the inverse problem determines the flux penetrating through the associated boundary elements, the camber line inclination correction $\delta\vartheta$ is given by:

$$\delta\vartheta = 0.5[\tan^{-1}(\frac{V_n}{V_t})^+ + \tan^{-1}(\frac{V_n}{V_t})^-] \tag{2.3}$$

Using this, the camber line rectification is performed iteratively. For the 2D incompressible potential flow, the complex potential $\phi + i\psi$ is an analytical function of $x + iy$, the panel method using the multiform singularities distribution described in [4] was used firstly to solve the inverse problem with success, this confirms that the boundary problem is correctly formulated. Figure 3 shows the initial and the final shape of a blade designed with adapted leading edge and with an appropriate loading distribution to prevent the boundary layer separation.

3. MERIDIONAL FLOW, S2 APPROACH.

In the first step, the vortex distribution is transformed into an axisymmetric one by spreading it in the azimuthal direction, this situation is equivalent to the case where the number of blades in the rotor or in the stator is assumed to be ∞, the flow field becomes also axisymmetric and can be analyzed in a meridional plan. Let ξ^1, $\xi^2 = \theta$, and ξ^3 represent the body fitted curvilinear coordinates (Fig. 4), the meridional velocity is represented by: $\vec{U} = V^1\vec{e}_1 + V^3\vec{e}_3 = W^1\vec{e}_1 + W^3\vec{e}_3$, the continuity equation becomes:

$$\frac{1}{\sqrt{\tilde{g}}}[\frac{\partial \sqrt{\tilde{g}}\rho U^1}{\partial \xi^1} + \frac{\partial \sqrt{\tilde{g}}\rho U^3}{\partial \xi^3}] = 0 \tag{3.1}$$

where $\tilde{g}$ represents the determinant of the modified metric tensor due to the flow channel striction produced by the thickness of the blades. Indeed, $\sqrt{g}$ represents the volume of the elementary cube: $(\vec{e}_3 \times \vec{e}_1) \cdot \vec{e}_2$, in the free space $|\vec{e}_2| = \sqrt{g_{22}} = r$, and in the blade row space the thickness of the blade reduces the flow channel, if $r\delta\theta_e$ denotes the thickness measured in the peripheral direction, N_b the number of blades in the rotor or stator, the modified element $\tilde{g}_{22}$ of the metric tensor is determined by:

$$\tilde{g}_{22} = (1 - \frac{N_b \delta\theta_e}{2\pi})^2 r^2$$

$\sqrt{\tilde{g}}$ simulating the elementary volume with striction in (3.1) is evaluated with $\tilde{g}_{22}$. Using the stream function

Third International Conference on Inverse Design Concepts and Optimization in Engineering Sciences (ICIDES-III), Editor: G.S. Dulikravich, Washington D.C., October 23-25, 1991

$\bar{\psi}$ to represent the flow field by imposing:

$$U^1 = \frac{1}{\sqrt{\rho g}} \frac{\partial \psi}{\partial \xi^3} \qquad \text{et} \qquad U^3 = -\frac{1}{\sqrt{\rho g}} \frac{\partial \psi}{\partial \xi^1} \tag{3.2}$$

the equation (3.1) is satisfied automatically. The governing equation for ψ is obtained by writing $\nabla \times \vec{U} = \Omega^2 \vec{e}_2$, where Ω^2 represents the azimuthal component of $\nabla \times \vec{V}$, it is deduced from the hub to shroud equilibrium condition. Let

$$H = \frac{P}{\rho} + \frac{V^2}{2} = \frac{P_t}{\rho} \qquad \text{and} \qquad I = \frac{P}{\rho} + \frac{W^2}{2} - \frac{\omega^2 r^2}{2} = H + \omega (V_\theta r)$$

The momentum equation is:

$$\vec{\Omega} \times \begin{cases} \vec{V} \\ \vec{W} \end{cases} = \begin{cases} -\nabla H \\ -\nabla I \end{cases} + \frac{\vec{F}_b}{\rho} + \frac{\vec{F}_d}{\rho} \qquad \begin{cases} \text{stator} \\ \text{rotor} \end{cases} \tag{3.3}$$

In fact, there is a pressure gradient in the azimuthal direction in the flow space between blades, in the axial symmetric S2 flow where the number of blades is supposed infinite, this pressure gradient disappears and the volume force $\vec{F}_b/\rho$ due to the blades has to be added in the momentum equation. The loss scheme [2] related to the plausible value of efficiency η for each streamline of the stage is added, this scheme suggests that the dissipative force $\vec{F}_d/\rho$ is related to the variation de $V_\theta r$ via η:

$$\frac{\vec{F}_d}{\rho} = \begin{cases} (\eta - 1) \frac{\omega}{(V)^2} [\vec{V} \cdot \nabla (V_\theta r)] \vec{V} & \text{stator} \\ (1 - \eta) \frac{\omega}{(W)^2} [\vec{W} \cdot \nabla (V_\theta r)] \vec{W} & \text{rotor} \end{cases} \tag{3.4}$$

$\vec{F}_d = 0$ as well as $\vec{F}_b = 0$ are imposed in the free space. Figure 5 shows the relation between the kinetic moment distribution in the blade row space and the circulation of the bound vortices produced by the blades. Let Γ_ψ denote the circulation generated by the blade in the section cut by an axisymmetric stream surface $\psi = cte$, the kinetic moment $(V_\theta r)_{m,k}$ generated by the bound vortices located between the leading edge and the abscissa m can be represented by:

$$(V_\theta r)_{m,\psi} = (V_\theta r)_{le,\psi} + \frac{N_b}{2\pi} \Gamma_\psi f(m, \psi) \tag{3.5}$$

Using (3.4) and adopting that $\partial I / \partial \xi^2$ or $\partial H / \partial \xi^2$ being equal to $-(F_d)_2/\rho$ in the dissipative scheme, the azimuthal component of the momentum equation leads to:

$$\frac{(F_b)_2}{\rho} = \left[V^1 \frac{\partial (V_\theta r)}{\partial \xi^1} + V^3 \frac{\partial (V_\theta r)}{\partial \xi^3} \right] \tag{3.6}$$

where $W_2 = V_\theta r + \omega r^2$ and $V_2 = V_\theta r$. The coordinates system ξ^i is chosen so that the constant ξ^3 lines are iteratively replaced by the streamlines. The component following $\vec{e}^3$ of the momentum equation represents the hub to shroud equilibrium condition, which gives:

$$\sqrt{g} \Omega^2 = \frac{1}{V^1} \left[\begin{cases} \frac{\partial I}{\partial \xi^3} + W^2 \sqrt{g} \Omega^1 \\ \frac{\partial H}{\partial \xi^3} + V^2 \sqrt{g} \Omega^1 \end{cases} - \frac{(F_b)_3}{\rho} - \frac{(F_d)_3}{\rho} \right] \qquad \begin{cases} \text{rotor} \\ \text{stator} \end{cases} \tag{3.7}$$

Let $\vec{n}$ design the normal of the camber surface of the blade, we have:

$$\vec{n} = n_1 \vec{e}^1 + n_2 \vec{e}^2 + n_3 \vec{e}^3$$

As $\vec{W} \perp \vec{n}$ in the rotor and $\vec{V} \perp \vec{n}$ in the stator, we have:

$$W^2 \quad \text{or} \quad V^2 = -\left(\frac{n_1}{n_2} V^1 + \frac{n_3}{n_2} V^3 \right)$$

and $\vec{F}_b \parallel \vec{n}$, we have:

$$\frac{(F_b)_2}{n_2} = \frac{(F_b)_3}{n_3}$$

Third International Conference on Inverse Design Concepts and Optimization in Engineering Sciences (ICIDES-III), Editor: G.S. Dulikravich, Washington D.C., October 23-25, 1991

Using (3.4), (3.6) and the last 3 relations, (3.7) becomes:

$$\sqrt{g}\Omega^2 = \frac{1}{V^1}\left\{ \begin{matrix} \frac{\partial I}{\partial \xi^3} \\ \frac{\partial H}{\partial \xi^3} \end{matrix} + \frac{n_1}{n_2}\frac{\partial (V_\theta r)}{\partial \xi^3} - \frac{n_3}{n_2}\frac{\partial (V_\theta r)}{\partial \xi^1} \right.$$
$$\left. - \begin{cases} (1-\eta)\frac{\bar{W}}{(\bar{W})^2} \\ (\eta-1)\frac{\bar{W}}{(\bar{V})^2} \end{cases} \frac{V_3}{V^1}\left[V^1\frac{\partial (V_\theta r)}{\partial \xi^1} + V^3\frac{\partial (V_\theta r)}{\partial \xi^3}\right] \right. \qquad \begin{cases} \text{rotor} \\ \text{stator} \end{cases} \tag{3.8a}$$

In the free space, the component following $\bar{e}^3$ of the momentum equation leads directly to:

$$\text{free space} \qquad \sqrt{g}\Omega^2 = \frac{1}{V^1}\left\{\frac{\partial H}{\partial \xi^3} - \frac{(V_\theta r)}{r^2}\frac{\partial (V_\theta r)}{\partial \xi^3}\right\} \tag{3.8b}$$

The dot product of the momentum equation with $\bar{V}$ in the stator and in the free space or with $\bar{W}$ in the rotor leads to the following relations which serve to update the nodal values of H or I:

$$\begin{cases} \text{free space} \\ \text{stator} \end{cases} \qquad \frac{\partial H}{\partial m} = \begin{cases} 0 \\ (\eta-1)\omega\dfrac{\partial (V_\theta r)}{\partial m} \end{cases} \tag{3.9a}$$

$$\text{rotor} \qquad \frac{\partial I}{\partial m} = (1-\eta)\omega\frac{\partial (V_\theta r)}{\partial m} \tag{3.9b}$$

where $\partial(\ )/\partial m$ denotes the meridional streamwise tangential derivative. Writing $\nabla \times \bar{U} = \Omega^2 \bar{e}_2$, we obtain the governing equation of ψ:

$$\frac{\partial}{\partial \xi^3}\left(\frac{g_{11}}{\rho\sqrt{g}}\frac{\partial \psi}{\partial \xi^3}\right) + \frac{\partial}{\partial \xi^1}\left(\frac{g_{33}}{\rho\sqrt{g}}\frac{\partial \psi}{\partial \xi^1}\right)$$
$$- \frac{\partial}{\partial \xi^3}\left(\frac{g_{13}}{\rho\sqrt{g}}\frac{\partial \psi}{\partial \xi^1}\right) - \frac{\partial}{\partial \xi^1}\left(\frac{g_{31}}{\rho\sqrt{g}}\frac{\partial \psi}{\partial \xi^3}\right) = \sqrt{g}\Omega^2 \tag{3.10}$$

For the inverse problem, the distribution of $V_\theta r$ is assigned, using (3.8), Ω^2 is updated iteratively. Let the camber surface of the blade be defined by $\theta = \xi^2(\xi^1, \xi^3) + cte$, if the coordinate lines $\xi^3 = cte$ are updated to the streamlines iteratively, ξ^2 can be computed using the slip condition:

$$\xi^2 = \xi^2_{i_e} + \int_{\xi^1_{i_e}}^{\xi^1} \frac{U^2}{U^1} d\xi^1 \tag{3.11}$$

Figure 5 shows the geometry of the blading of a multistage turbopump obtained by solving the inverse problem. The CPU time on IBM 3090 in scalar mode is about 1 minute for the entire turbopump. The grid used for the S2 computation is 300×16. Figure 6 shows the comparison of the centrifugal impellers designed with $\eta = 1$ and $\eta < 1$ having the same level of total pressure gain.

Blade surface pressure evaluation. – Usually the S2 approach leads to the determination of the mean velocity on both faces of the blade:

$$\begin{cases} \text{rotor} \\ \text{stator} \end{cases} \qquad \begin{matrix} W \\ V \end{matrix} = \left[g_{11}V^1V^1 + 2g_{13}V^1V^3 + g_{33}V^3V^3 + \begin{matrix} g_{22}(V_\theta r + \omega r^2)^2 \\ g_{22}(V_\theta r)^2 \end{matrix}\right]^{1/2} \tag{3.12}$$

Let ΔU denote the difference of the absolute velocities $(V^+ - V^-)$ or the relative velocity $(W^+ - W^-)$ on the two faces of the blade, when the number of blades is finite, this difference is related to the local density of bound vortex generated by the blade. In the S2 scheme, consider the blade section cut by a $\xi^3 = cte$ surface, the flux of bound vortices generated by the element $\delta\xi^1$ of the blade is determined by the flux of $\bar{\Omega}$ through the elementary surface $(\delta S)_3\bar{e}^3 = \sqrt{g}\delta\xi^1\delta\xi^2\bar{e}^3$, where $\delta\xi^2$ should be equal to $2\pi/N_b$. Using the Stokes relation that implies the circulation produced by ΔU is equal to the flux of the bound vortices we get the following relation:

$$(\Delta U)_{i,k} = \frac{2\pi}{N_b}\frac{cos\beta}{\sqrt{g_{11}}}\left|[V_\theta r]^{i+1/2,k}_{i-1/2,k}\right| \tag{3.13}$$

where β denotes the local angle of the blade section with respect to the meridional plane. (3.12) and (3.13) are used to compute surface velocity on both faces of the blades, then the pressure distribution by the S2 approach can be deduced. (Fig. 9)

4. BLADE TO BLADE FLOW, S1 APPROACH.

The blade to blade flow confined in each axisymmetric stream sheet is analyzed in order to define the final geometry for each section of the blade and to obtain the pressure distribution. At the beginning, the contour of the blade is created from the camber line obtained from the S2 step with the assigned thickness distribution. The conformal mapping $(m,\theta) \Longrightarrow (x^1,x^2)$:

$$\begin{cases} x^1 = r_o \int_{m_o}^{m} \dfrac{dm}{r} \\ x^2 = r_o(\theta - \theta_o) \end{cases} \tag{4.1}$$

transforms the blade to blade flow confined in an axisymmetric stream sheet into a 2D cascade flow in the (x^1,x^2) plane. The body fitted coordinate system constituted by the equipotential lines $\xi^1 = cte$ and the streamlines $\xi^2 = cte$ of a fictive 2D flow around the cascade is created using the panel method [4]. In this system, the continuity equation becomes:

$$\frac{1}{\sqrt{g}}\Big[\frac{\partial}{\partial \xi^1}(\rho\sqrt{g}\,U^1) + \frac{\partial}{\partial \xi^2}(\rho\sqrt{g}\,U^2)\Big] = 0 \tag{4.2}$$

where U^i represent the contravariant components of the absolute velocity $\vec{V}$ for the stator and relative velocity $\vec{W}$ for the rotor and

$$\sqrt{g} = \frac{D(x^1,x^2)}{D(\xi^1,\xi^2)}\Big(\frac{r}{r_o}\Big)^2\tau$$

where $D(x^1,x^2)/D(\xi^1,\xi^2)$ denotes the Jacobian, τ represents the local thickness of the stream sheet. Introducing the stream function ψ with

$$\begin{cases} U^1 = \dfrac{1}{\rho\sqrt{g}}\dfrac{\partial \psi}{\partial \xi^2} \\ U^2 = -\dfrac{1}{\rho\sqrt{g}}\dfrac{\partial \psi}{\partial \xi^1} \end{cases} \tag{4.3}$$

(4.2) is satisfied. From the momentum equation, we can show that the free vortex of the absolute velocity shedding from the preceeding blade row must be tangential to the axisymetric stream sheet, the governing equation of the blade to blade flow stream function is deduced from this condition: for the relative flow around the blades of the rotor, we have:

$$-\Big[\frac{\partial}{\partial \xi^1}\Big(\frac{g_{22}}{\rho\sqrt{g}}\frac{\partial \psi}{\partial \xi^1}\Big)+\frac{\partial}{\partial \xi^2}\Big(\frac{g_{11}}{\rho\sqrt{g}}\frac{\partial \psi}{\partial \xi^2}\Big)\Big] = - \frac{\partial g_{21}W^1}{\partial \xi^1} + \frac{\partial g_{12}W^2}{\partial \xi^2} + 2\sqrt{g}\frac{\omega r}{\tau}\frac{d\,\log r}{dm} \tag{4.4}$$

Boundary conditions for the inverse problem:

$$\begin{cases} \text{Flux conservation:} & [\psi]_-^+ = 0 \\ \text{Bound vorticity assigned:} & \big[W_1 d\xi^1 - \omega r^2 d\theta\big]_-^+ = \Gamma df \end{cases} \tag{4.5}$$

The solution of the inverse problem leads to the determination of flux penetration on the blade contour, the camber line inclination correction $\delta\vartheta$ is given by:

$$\delta\vartheta = 0.5\Big[\tan^{-1}\Big(\frac{\sqrt{g}}{\tau}\frac{W^2}{W_1}\Big)^+ + \tan^{-1}\Big(\frac{\sqrt{g}}{\tau}\frac{W^2}{W_1}\Big)^-\Big] \tag{4.6}$$

Figure 7 shows the network (ξ^1, ξ^2) around a blade row for an impeller. Figure 8 shows the comparison of the camber lines of the impeller obtained from the S2 approach and rectified by the S1 approach. Figure 9 shows the pressure distributions obtained from the S2 and S1 approaches. For the case of the turbopump, the loading is optimised to avoid the cavitation. The results from the S2 and S1 computations are similar, but not identical, the need of the S1 computation to obtain the final geometry definition of the blades is confirmed. For one stream sheet, the CPU time on a IBM workstation RISC 6000/320 is about 40 minutes, or about 5 minutes on IBM 3090 in scalar mode. The grid used is 150×16.

5. CONCLUSION.

The representation of the blades by the vortex distribution enables the formulation of the well-posed inverse problem, and which leads to design the blading of a turbomachine. The two steps S2 – S1 quasi-3D approach has been applied on different axial and radial geometries. Several kinds of loading function have been tried. The results show that the success of the blading design depends greatly on the meridional $(V_\theta r)$ distribution assignment associated with the loss distribution. To optimise the design in order to avoid the formation of the cavitation or the separation of the boundary layer in the design condition, when the loading is not too high, experiences show that an adequate modification of the bound vortices distribution function f may effectively lead to prevent the surface pressure to be lower than the cavitation level or to maintain the adverse pressure gradient below the boundary layer separation criterion. The inverse problem procedure has been elaborated to calculate the turbomachines in incompressible range, the research works are planning to extend this method to make the transonic designs.

ACKNOWLEDGEMENT

This work was supported by a research contract from the SEP (Société Européenne de Propulsion). The authors wish to thank them for their cooperation to this publication.

REFERENCE

1. Wu C.H., "A general theory of three dimensional flow in subsonic and supersonic turbomachines of axial, radial and mixed flow type. NACA TN 2604, 1952

2. Horlock J.H., "On Entropy Production in Adiabatic Flow in Turbomachines." Journal of Basic Engineering, Trans. ASME, Dec. 1971.

3. Luu T.S., and Viney B., "The Turbomachine Blading Design Achieved by Solving the Inverse Problem." ASME Paper No.87-GT-215.

4. Luu T.S., Coulmy G., and Viney B., "Design problem of the profile or cascade of profiles and construction of the orthogonal networks using the Riemann surface for the multiform singularities." Computational Mechanic (1989) 4, 309-317.

Third International Conference on Inverse Design Concepts and Optimization in Engineering Sciences
(ICIDES-III), Editor: G.S. Dulikravich, Washington D.C., October 23-25, 1991.

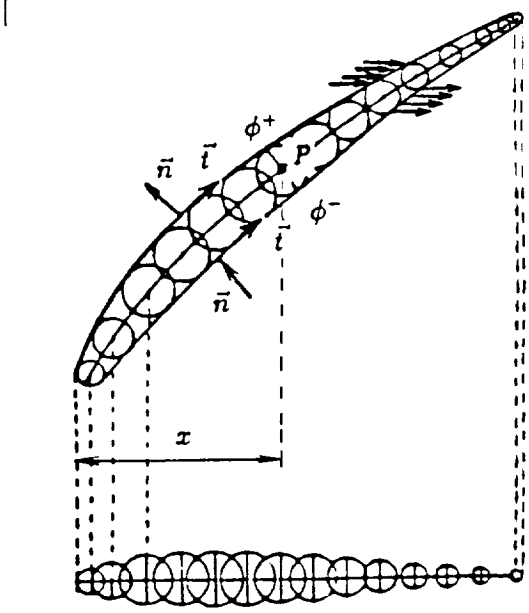

Fig. 1. Associated elements on both sides of the blade and on the camber line.

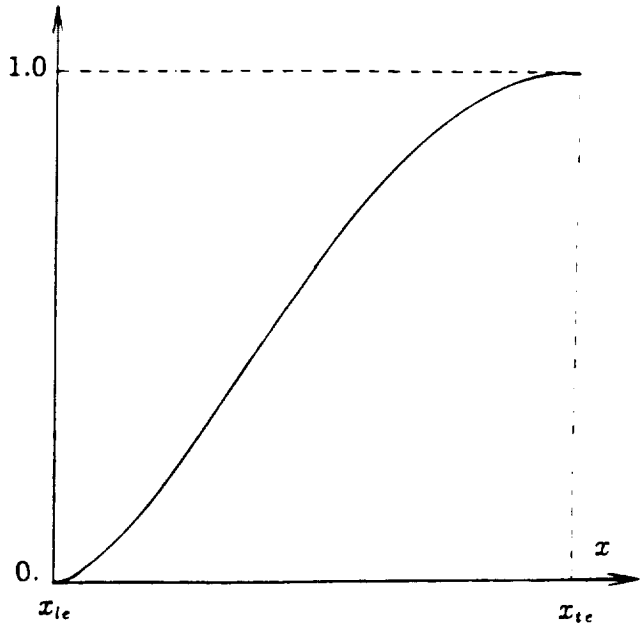

Fig. 2. Typical loading function $f(x)$.

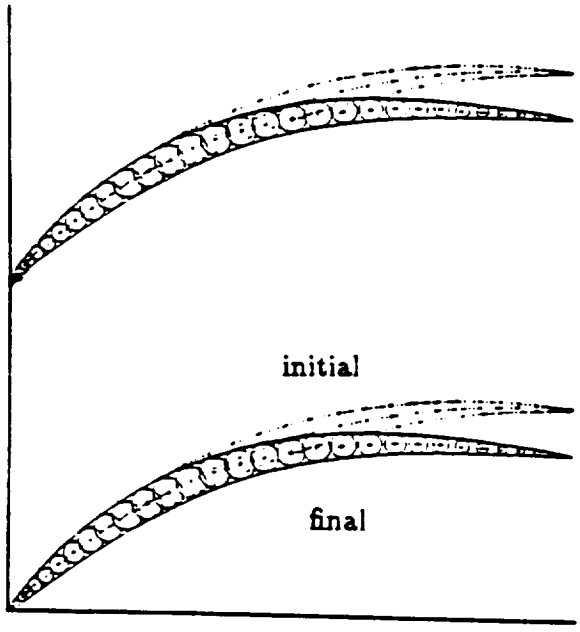

Fig. 3. Initial and final shape of the blade.

Third International Conference on Inverse Design Concepts and Optimization in Engineering Sciences (ICIDES-III), Editor: G.S. Dulikravich, Washington D.C., October 23-25, 1991.

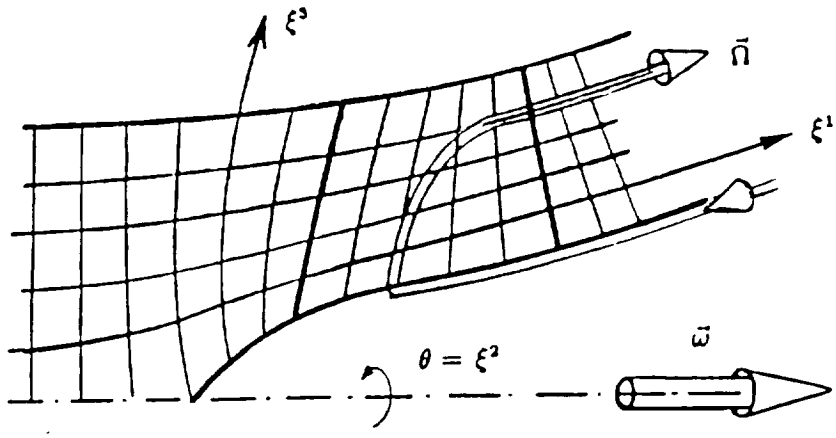

Fig. 4. Boby fitted coordinate system ξ^1, $\xi^2 = \theta$, ξ^3.

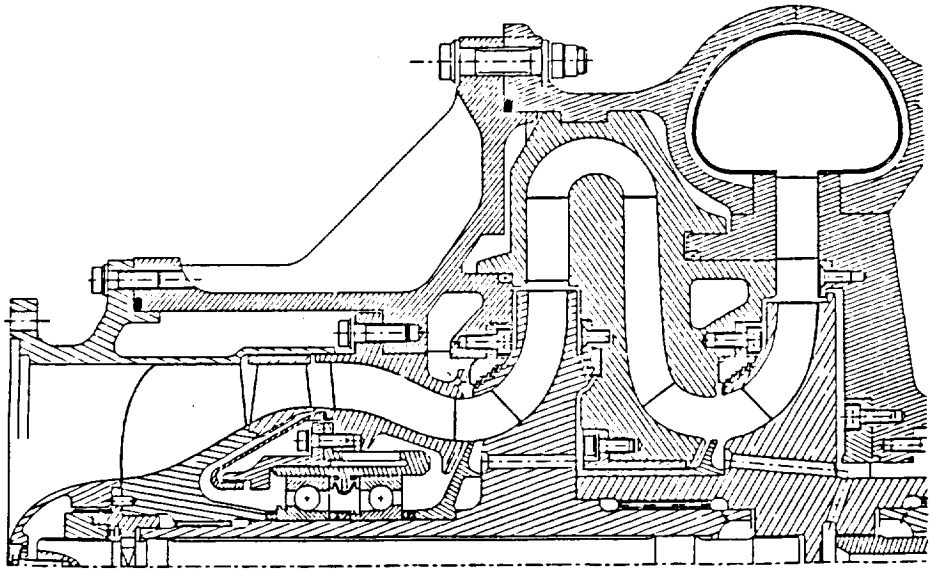

Meridional section of a multistage turbopump.

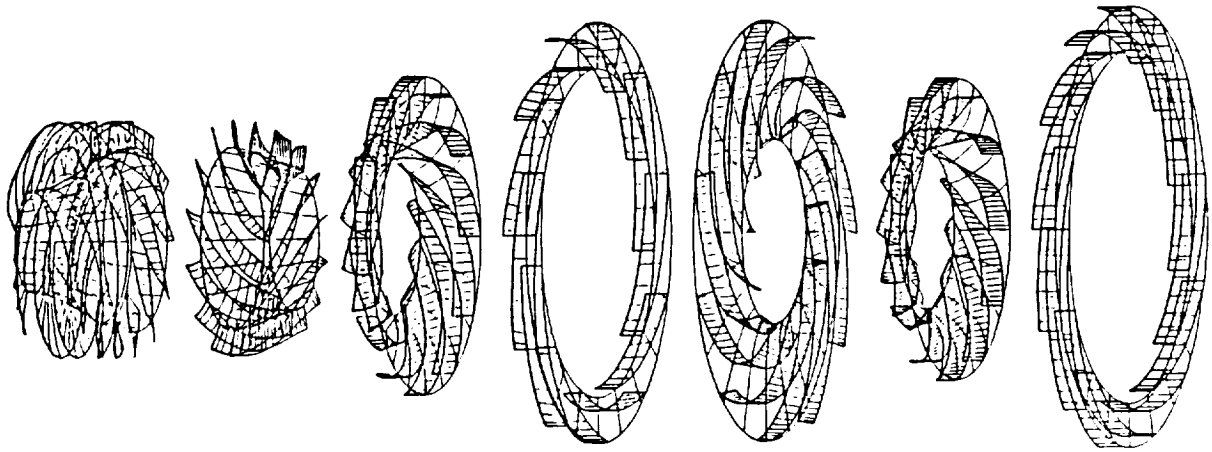

The blading obtained by the S2 inverse solution.

Fig. 5. The blading of a multistage turbopump.

Third International Conference on Inverse Design Concepts and Optimization in Engineering Sciences (ICIDES-III), Editor: G.S. Dulikravich, Washington D.C., October 23-25, 1991.

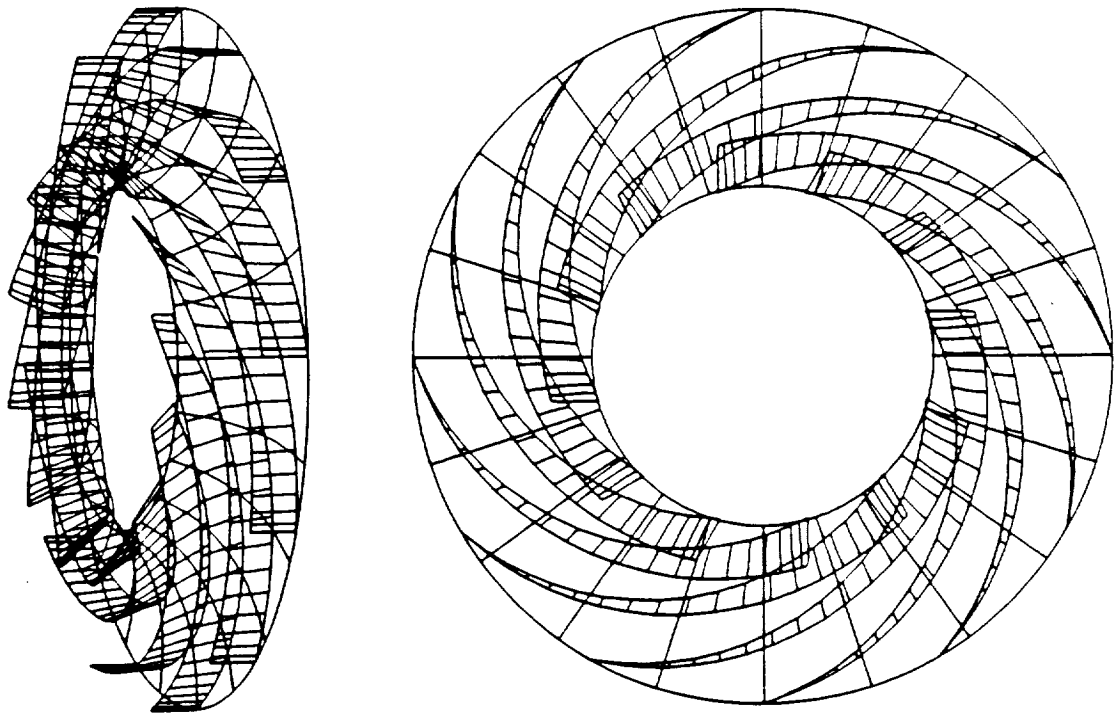

$\eta = 1$

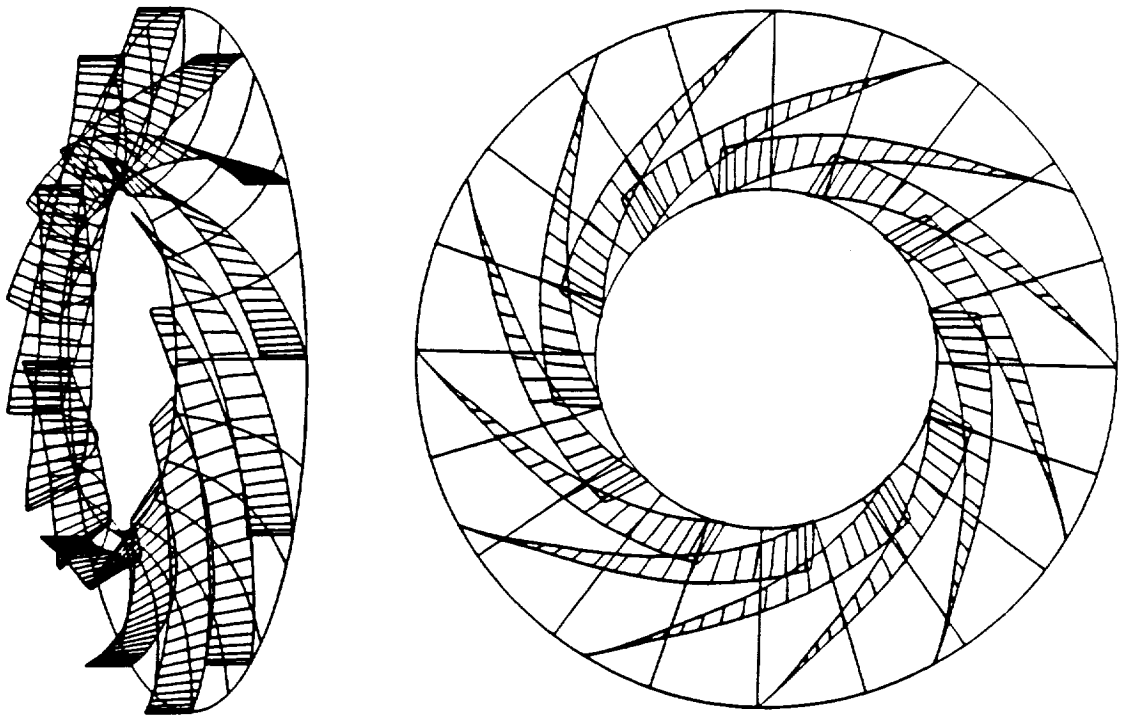

$\eta = 0.7$

Fig. 6. Centrifugal impellers designed with $\eta = 1$ and $\eta < 1$ having the same level of total pressure gain.

Third International Conference on Inverse Design Concepts and Optimization in Engineering Sciences
(ICIDES-III), Editor: G.S. Dulikravich, Washington D.C., October 23-25, 1991.

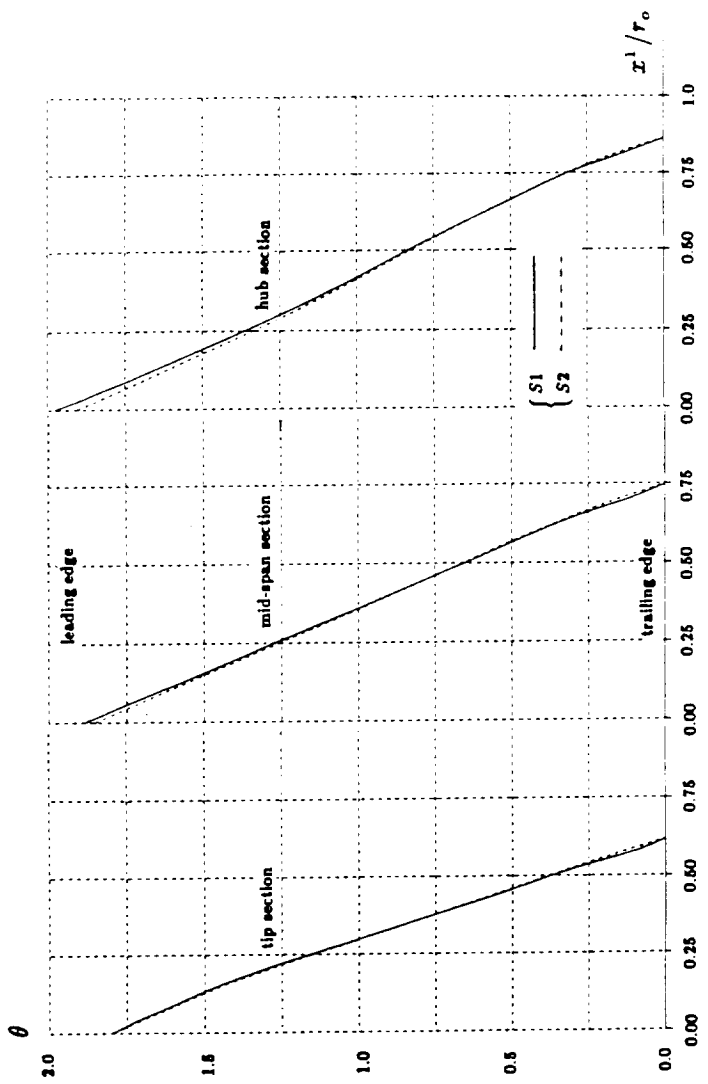

Fig. 8. Camber lines of the impeller obtained from S2-S1 approaches.

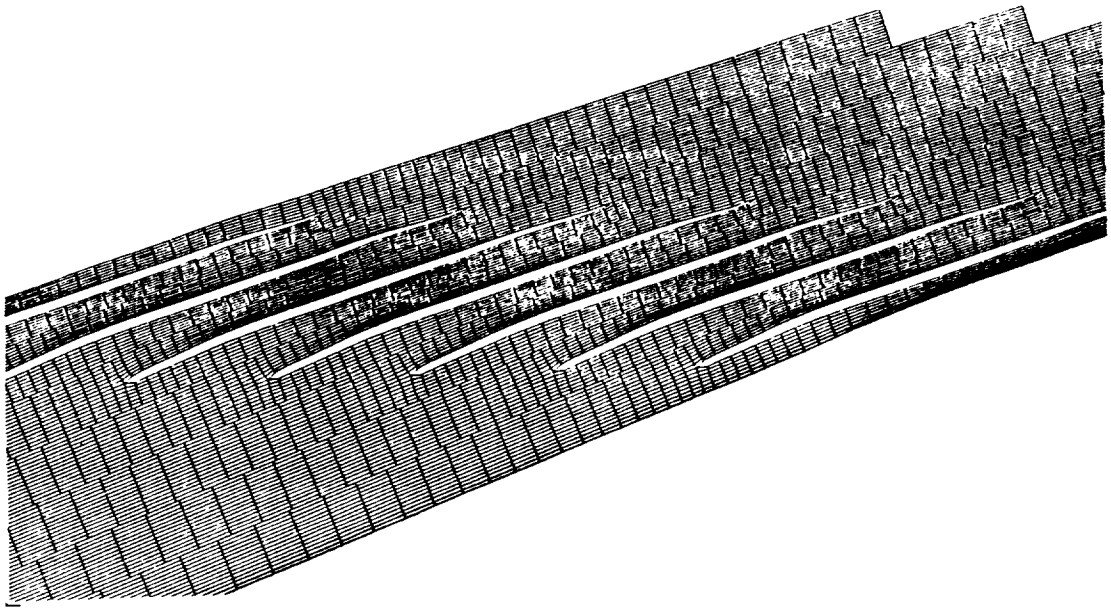

Fig. 7. Network (ξ^1, ξ^2) around a blade row in the (x^1, x^2) plane.

Third International Conference on Inverse Design Concepts and Optimization in Engineering Sciences
(ICIDES-III), Editor: G.S. Dulikravich, Washington D.C., October 23-25, 1991.

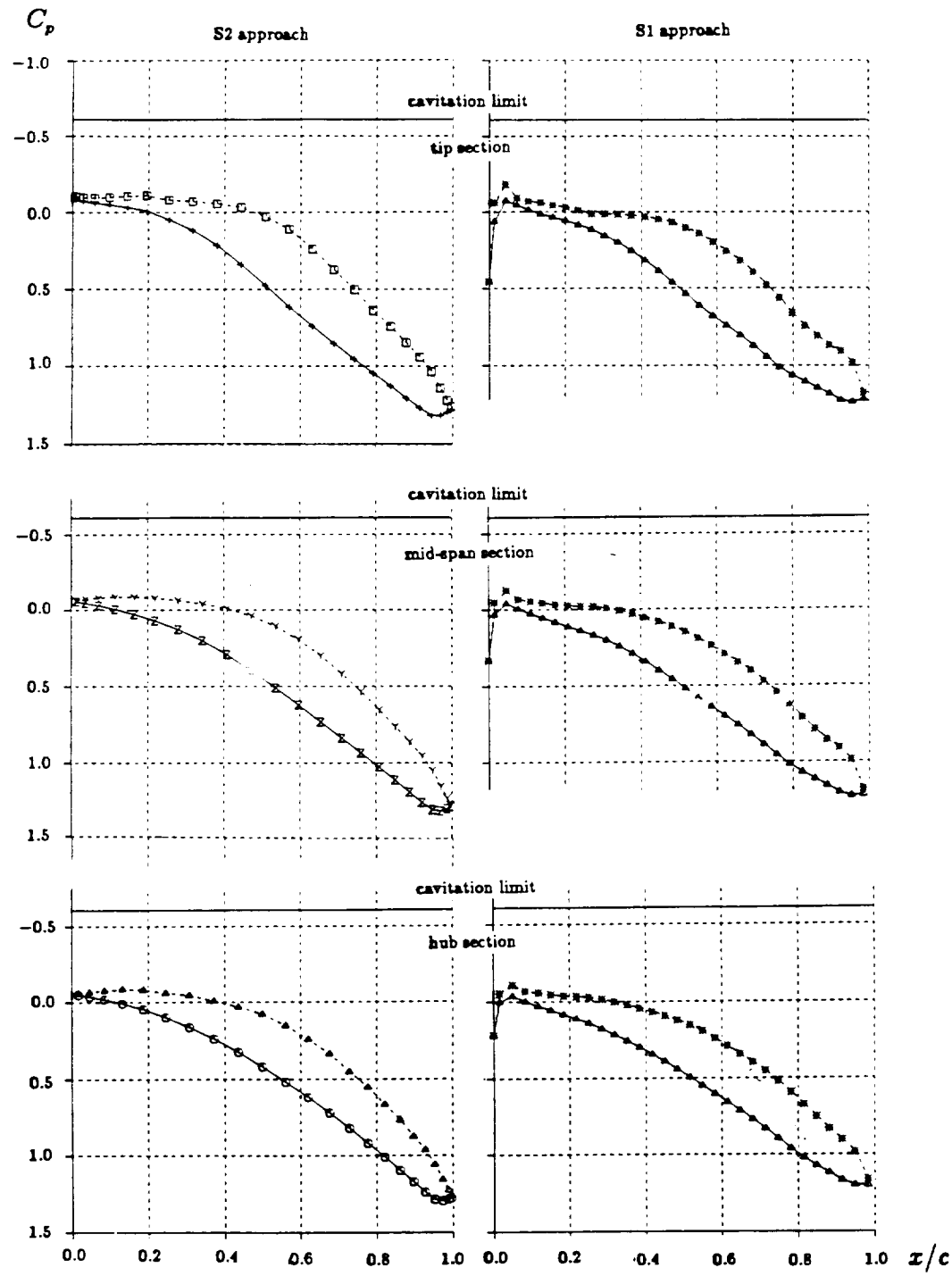

Fig. 9. Pressure distribution for 3 sections of the impeller from S2-S1 approaches.